Spectroscopic Determination of the Ring-Twisting Potential Energy Function of 1,3-Cyclohexadiene and Comparison with Ab Initio Calculations

Daniel Autrey, Jaebum Choo,† and Jaan Laane*

Department of Chemistry, Texas A&M University, College Station, Texas 77843-3255

Received: June 6, 2001; In Final Form: August 13, 2001

The high-temperature vapor-phase Raman spectrum of 1,3-cyclohexadiene shows nine transitions resulting from the ν_{19} (A_2) twisting mode (labeled according to C_{2v} symmetry). Ab initio calculations predict barriers in the 1197−1593 cm^{-1} range. Far-infrared absorption bands confirm five of these transitions. A one-dimensional potential energy function with a barrier of 1132 cm^{-1} does an excellent job of fitting the data. Other Raman and infrared combination bands also verify the assignments and provide information on the vibrational coupling. The twisting angles were determined to be 9.1° and 30.1°. Vibrational frequencies calculated by ab initio methods generally give good agreement with all of the experimental values.

Introduction

It is generally agreed that 1,3-cyclohexadiene is nonplanar and possesses C_2 symmetry. This is based on microwave,[1,2] electron diffraction,[3−5] and Raman studies[6] as well as ab initio calculations.[7,8] However, considerable disparity exists between the various experimentally determined and theoretically calculated structural parameters, particularly the dihedral angles. The inversion barrier (barrier to planarity) has been reported in a Raman study[6] to be 1099 cm^{-1}, but this was based on only four observed transitions so the barrier value had to be attained by extrapolation. The most recent ab initio calculation[8] predicted a barrier of 1295 cm^{-1}.

Many years ago Laane and Lord demonstrated that molecules such as cyclopentene[9] and 1,4-cyclohexadiene[10] could be considered to be "pseudo-four-membered rings" in regard to their out-of-plane ring modes. If two carbon atoms joined by a double bond are assumed to move together, then the out-of-plane vibrations of these molecules resemble the ring-puckering vibrations of four-membered ring molecules such as cyclobutane. This also applies to 1,3-cyclohexadiene so that its lowest frequency vibration can be represented by a one-dimensional model where this out-of-plane vibration is assumed to be separated from all the other vibrational modes. Carreria et al.[6] made this assumption in their Raman work, and they used a reduced (dimensionless) vibrational potential energy function

$$V = A(Z^4 + BZ^2) \quad (1)$$

of the type described by Laane[11] to fit the observed Raman data. However, no attempts were made to calculate the kinetic energy (reciprocal reduced mass) function, which is required if structural information is to be obtained. Hence, the dihedral angles for the molecule could not be determined.

In this study we report an improved vapor-phase Raman spectrum of 1,3-cyclohexadiene recorded at high-temperature showing a total of nine observed transition frequencies. We also report the first observations of the far-infrared spectra and mid-infrared and Raman combination bands for this molecule. The spectra were analyzed using an appropriately computed kinetic energy model to determine the potential energy function and to accurately calculate the inversion barrier and the dihedral angles of twisting for the molecule. Our methodology for determining the vibrational potential energy surfaces using low-frequency vibrational spectroscopy has been summarized in several reviews.[12−16]

Experimental Section

The sample of 1,3-cyclohexadiene was purchased from Aldrich Chemical Co. (97% purity) and purified by vacuum distillation.

Far-infrared spectra of the vapor were recorded on a Bomem DA8.02 Fourier transform infrared interferometer equipped with a DTGS/POLY detector. The sample was contained in a 4.2 m multipass cell fitted with polyethylene windows, which had been pounded with a ballpeen hammer to eliminate interference fringes. A 12-μm-thick Mylar beamsplitter was used with a glowbar source to record spectra in the 100−400 cm^{-1} region. Typically, 5000−8000 scans at 0.25 cm^{-1} resolution were obtained. Vapor-phase mid-infrared spectra were also recorded on the Bomem DA8.02 Fourier transform infrared interferometer. The sample was contained in a 20 m multipass cell fitted with KBr windows.

Raman spectra of the vapor at temperatures between 120 and 160 °C were recorded using an Instruments SA JY-U1000 spectrometer and a Coherent Radiation Innova 20 argon ion laser with excitation at 514.5 nm and 4-W laser power. Both a photomultiplier tube and a liquid nitrogen cooled charge-coupled device were used as detectors. Spectral resolutions in the 0.5−2.0 cm^{-1} range with the photomultiplier tube and 0.7 cm^{-1} with the charge-coupled device were used. The sample was contained in a high-temperature Raman cell previously described.[17] Sample pressures were typically 700 Torr.

Vibrational Model and Kinetic Energy Expansion

Figure 1 shows the three out-of-plane ring modes of 1,3-cyclohexadiene, labeled for an assumed planar (C_{2v}) structure. The ν_{19} ring-twisting mode of A_2 symmetry is the vibration of

* Corresponding author.
† Permanent address: Department of Chemistry, Hanyang University, Hanyang, 425-791 Ansan, Korea.

10.1021/jp012170j CCC: $20.00
Published on Web 10/23/2001

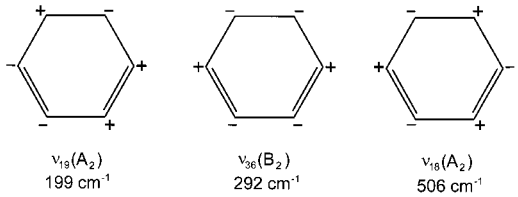

Figure 1. Out-of-plane ring modes of 1,3-cyclohexadiene. The vibrational numbering is based on C_{2v} symmetry. + = above plane; − = below plane.

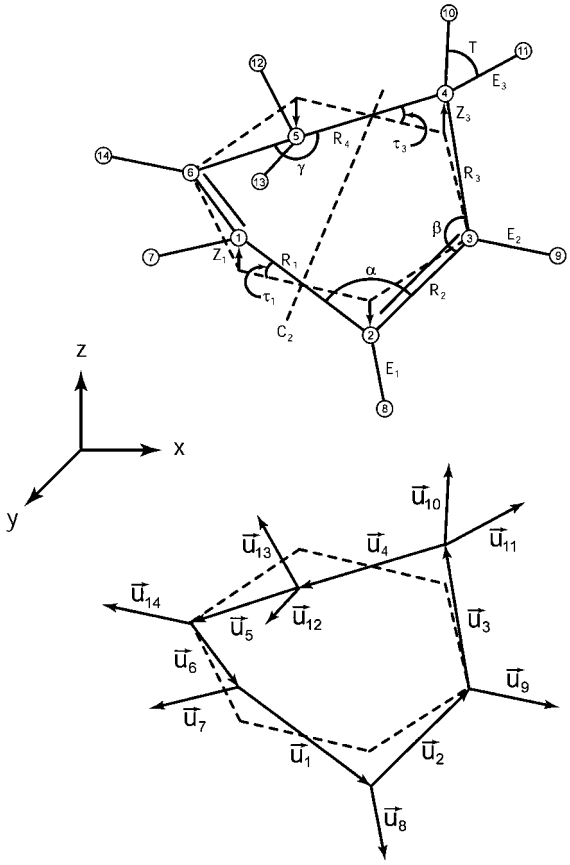

Figure 2. Structural parameters for 1,3-cyclohexadiene (top). Vectors used to define atom positions as a function of τ_1 and τ_3 (bottom).

primary interest and it is assumed to be separable from the ν_{36} (different symmetry) and ν_{18} (higher frequency) modes.

The calculation of the kinetic energy expression for the ν_{19} ring-twisting mode requires a representation of the vibrational motion and a reasonable knowledge of the molecular bond lengths and angles. The structure used for the computations was obtained from ab initio calculations, which are described later. Figure 2 (top) shows the structural parameters for 1,3-cyclohexadiene, and Figure 2 (bottom) shows the vectors used to define the positions of each of the atoms during the ring-twisting vibration. The twisting angles τ_1 and τ_3 define the out-of-plane ring motion. As in our previous computations for the kinetic energy expressions[18−22] of the out-of-plane ring modes, the bond lengths were assumed to remain fixed and hydrogen atom positions were determined by the bisector model. (CCC angles and HCH angles have a common bisector, for example.) For the vibrational model it was necessary to know the relative magnitudes of the torsional angles τ_1 and τ_3. The ratio τ_3/τ_1 is taken from the ab initio calculations and a value of 3.273 was used. The normalized vibrational coordinate is then

$$\tau = 0.95637\tau_3 + 0.229217\tau_1 \qquad (2)$$

TABLE 1: Components of the Bond Vectors $\vec{u}_i = a_i\vec{i} + b_i\vec{j} + c_i\vec{k}$ for the Ring-Twisting Vibration of 1,3-Cyclohexadiene

i	a_i	b_i	c_i
1	X_{12}	0	$-2Z_1$
2	X_{23}	Y_{23}	Z_1
3	$-X_{34}$	Y_{34}	Z_3
4	$-X_{45}$	0	$-2Z_3$
5	$-X_{34}$	$-Y_{34}$	Z_3
6	X_{23}	$-Y_{23}$	Z_1
7	x_7	y_7	z_7
8	x_8	y_8	z_8
9	x_9	y_9	z_9
10	$p_{4x} + v_{4x}$	$p_{4y} + v_{4y}$	$p_{4z} + v_{4z}$
11	$p_{4x} - v_{4x}$	$p_{4y} - v_{4y}$	$p_{4z} - v_{4z}$
12	$p_{5x} + v_{5x}$	$p_{5y} + v_{5y}$	$p_{5z} + v_{5z}$
13	$p_{5x} - v_{5x}$	$p_{5y} - v_{5y}$	$p_{5z} - v_{5z}$
14	x_{14}	y_{14}	z_{14}

$$\tau_1 = \sin^{-1}\left[\frac{2Z_1}{R_1}\right];\ \tau_3 = \sin^{-1}\left[\frac{2Z_3}{R_3}\right]$$

$$X_{12} = \sqrt{R_1^2 - 4Z_1^2};\ X_{23} = -\frac{(R_1R_2\cos\alpha - 2Z_1^2)}{X_{12}}$$

$$Y_{23} = \sqrt{R_2^2 - Z_1^2 - X_{23}^2}$$

$$X_{34} = \frac{[2X_{23} + X_{12} - X_{45}]}{2};\ Y_{34} = \sqrt{R_3^2 - Z_3^2 - X_{34}^2}$$

$$\vec{u}_7 = x_7\vec{i} + y_7\vec{j} + z_7\vec{k} = r_1\left[\frac{\vec{u}_6}{R_6} - \frac{\vec{u}_1}{R_1}\right]/2\cos\frac{\alpha}{2}$$

$$\vec{u}_8 = x_8\vec{i} + y_8\vec{j} + z_8\vec{k} = r_1\left[\frac{\vec{u}_1}{R_1} - \frac{\vec{u}_2}{R_2}\right]/2\cos\frac{\alpha}{2}$$

$$\vec{u}_9 = x_9\vec{i} + y_9\vec{j} + z_9\vec{k} = r_2\left[\frac{\vec{u}_2}{R_2} - \frac{\vec{u}_3}{R_3}\right]/2\cos\frac{\beta}{2}$$

$$\vec{u}_{14} = x_{14}\vec{i} + y_{14}\vec{j} + z_{14}\vec{k} = r_2\left[\frac{\vec{u}_4}{R_4} - \frac{\vec{u}_5}{R_5}\right]/2\cos\frac{\beta}{2}$$

$$\vec{p}_4 = r_3\cos\frac{T}{2}\left[\frac{\vec{u}_3}{R_3} - \frac{\vec{u}_4}{R_4}\right]/2\cos\frac{\gamma}{2};\ \vec{v}_4 = \frac{r_3\sin\frac{T}{2}[\vec{u}_4 \times (-\vec{u}_3)]}{R_3R_4\sin\gamma}$$

$$\vec{p}_5 = r_3\cos\frac{T}{2}\left[\frac{\vec{u}_4}{R_4} - \frac{\vec{u}_5}{R_5}\right]/2\cos\frac{\gamma}{2};\ \vec{v}_5 = \frac{r_3\sin\frac{T}{2}[\vec{u}_5 \times (-\vec{u}_4)]}{R_4R_5\sin\gamma}$$

Table 1 defines the vectors shown in Figure 2 (bottom) in terms of τ_1 and τ_3. From these, the position of each atom as a function of τ can be calculated. This allows the derivatives necessary for the computation of the kinetic energy to be calculated (see refs 18−22). The coordinate dependent kinetic energy (reciprocal reduced mass) thus calculated for 1,3-cyclohexadiene is

$$g_{44} = 0.03490 - 0.0110\tau^2 - 0.01516\tau^4 + 0.01148\tau^6 \qquad (3)$$

The coordinate dependence of this function is shown in Figure 3.

Spectroscopic Results

Figure 4 shows the vapor-phase Raman spectra in the 125−600 cm^{-1} region. Bands due to all three out-of-plane ring modes (ν_{18}, ν_{19}, and ν_{36}) can be seen along with $\nu_{12}(A_1)$ and $\nu_{30}(B_1)$, which are described later. 1,3-Cyclohexadiene has C_2 symmetry but its vibrations can be better visualized using a C_{2v} (planar) model. The lowest frequency vibration gives rise to several bands between 100 and 200 cm^{-1}. The other two out-of-plane modes have B_2 and A_2 symmetry and are twisting motions about the C═C double bonds. These give rise to the Raman bands at

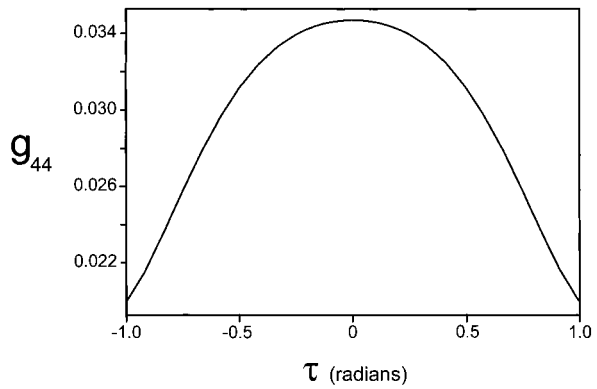

Figure 3. Coordinate-dependent kinetic energy (reciprocal reduced mass) for 1,3-cyclohexadiene.

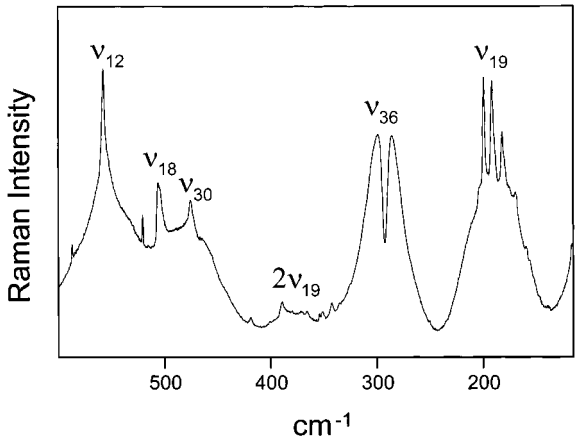

Figure 4. Vapor-phase Raman spectrum of 1,3-cyclohexadiene in the 125−600 cm^{-1} region showing the out-of-plane ring modes. 700 Torr, 120 °C.

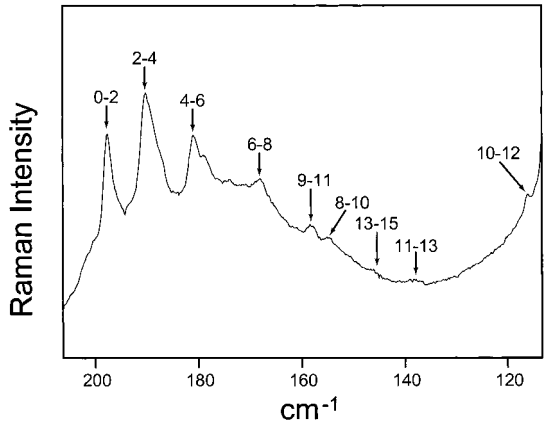

Figure 5. Vapor-phase Raman spectrum of 1,3-cyclohexadiene for the A_2 ring-twisting mode. 700 Torr, 120 °C.

292 and 506 cm^{-1}, respectively. The $\nu_{36}(B_2)$ mode has a corresponding type C infrared band with considerable infrared intensity, but no infrared absorption is seen for the A_2 mode (as expected). Di Lauro et al.[23] have previously assigned bands in the liquid Raman spectra at 201 and 298 cm^{-1} to these out-of-plane ring vibrations, but their 468 cm^{-1} assignment to ν_{18} is actually due to ν_{30}.

Figure 5 shows the vapor-phase Raman spectrum of 1,3-cyclohexadiene for the low-frequency A_2 mode (ν_{19}). The assignments of the transitions in terms of the ring-twisting quantum numbers are also shown. Nine transitions were assigned, whereas in the previous study only four bands were observed. As shown below, quantum states 12 and 13 are right at the top of the barrier and 15 is well above it. Hence, the data allow the shape of the potential function and its barrier to planarity (inversion barrier) to be determined accurately. Table 2 lists the observed frequencies.

TABLE 2: Observed and Calculated Frequencies for the ν_{19} (A_2) Mode of 1,3-Cyclohexadiene

	Raman			calculated[b]	
transition	lit.[a]	this work	far-infrared	frequency	Δ[c]
0−2	198	198	198.7	199.8	−1.1
2−4	190	190	191.1	191.3	−0.2
4−6	180	181	181.5	181.6	−0.1
6−8	167	168	169.6	169.6	0.0
8−10	—	155	—	152.6	2.4
9−11	—	158	157.9	155.1	2.9
10−12	—	116	—	117.3	−1.3
11−13	—	138	—	142.0	−4.0
12−14	—	—	—	105.3	—
13−15	—	146	—	145.5	0.6

[a] Reference 6. [b] $V = 1.845 \times 10^4\tau^4 - 9.138 \times 10^3\tau^2$. [c] $\nu_{CALC} - \nu_{OBS}$ where ν_{OBS} is the far-infrared value where available.

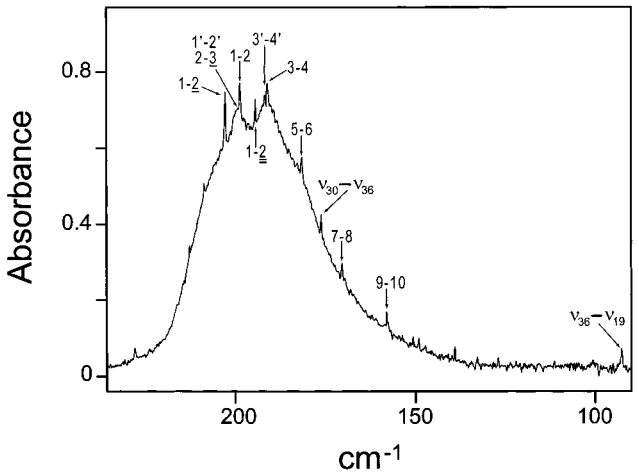

Figure 6. Far-infrared spectrum of 1,3-cyclohexadiene vapor. 90 Torr, 4.2 m path length, 25 °C. The ring-twisting transitions are labeled. A prime indicates ν_{36} excited state; an underline, ν_{30} excited state; and double underline, ν_{18} excited state.

With C_2 symmetry the ring-twisting vibration of 1,3-cyclohexadiene is totally symmetric with *A* symmetry species. Thus, this vibration is in principle both infrared and Raman allowed. However, in an assumed C_{2v} planar conformation, the vibration would have an A_2 representation which is infrared forbidden. Moreover, single quantum jumps for a C_{2v} molecule are expected to give rise to much weaker bands in Raman spectra than double quantum jumps, which are totally symmetric. (The polarized bands typically have considerably more intensity.) The nearness to C_{2v} symmetry thus explains why the Raman spectra (Figure 5) show the double quantum jumps. It also predicts that the transitions should be very weak in the infrared spectra since the A_2 bands in the C_{2v} approximation are forbidden. Figure 6, however, shows that in the far-infrared spectra this vibration gives rise to some weak absorption that can be observed with a long-path (4.2 m) cell. Several weak Q branches on top of a broad rotational background can be seen in the figure, and these frequencies agree well with the Raman values. These have been labeled as single quantum transitions (A_2 in the C_{2v} approximation) but could also be caused by the double quantum jump transitions (A_1 in the C_{2v} approximation), which are coincident due to inversion doubling. Observation of these infrared bands is advantageous as their frequencies are more accurately determined (±0.2 cm^{-1}) than those from the Raman spectra (±1.0 cm^{-1}). The labels in Figure 6 correspond to the quantum

TABLE 3: Combination and Overtone Bands (cm^{-1}) of 1,3-Cyclohexadiene

infrared sum bands

	$v_{19}+v_{36}$		$v_{19}+v_{30}$		$v_{19}+v_{33}$		
transition	$\bar{v}$	$\bar{v}-291.0$	$\bar{v}$	$\bar{v}-467.6$	$\bar{v}$	$\bar{v}-926.1$	far-infrared
1−2	489.8	198.8	670.8	203.2	1123.9	197.8	198.7
3−4	482.8	191.8	671.8	204.2	1114.6	188.5	191.1
5−6	472.8	181.8	668.5	200.9	1103.4	177.3	181.5
7−8	460.3	169.3	665.6	198.0	—	—	169.6

Raman overtones ($2v_{19}$)

transition	$\bar{v}$	inferred
0−4	389	388
2−6	372	371
4−8	351	349
6−10	325	323

other combinations

spectrum	band	observed	inferred
infrared	$v_{36}-v_{19}$	92.5	291.0 − 198.7 = 92.3
infrared	$v_{30}-v_{36}$	176.1	467.6 − 291.0 = 176.6
Raman	$v_{30}-v_{36}$	175	467.6 − 291.0 = 176.6
Raman	$v_{35}-v_{19}$	366	658.4 − 291.0 = 367.4

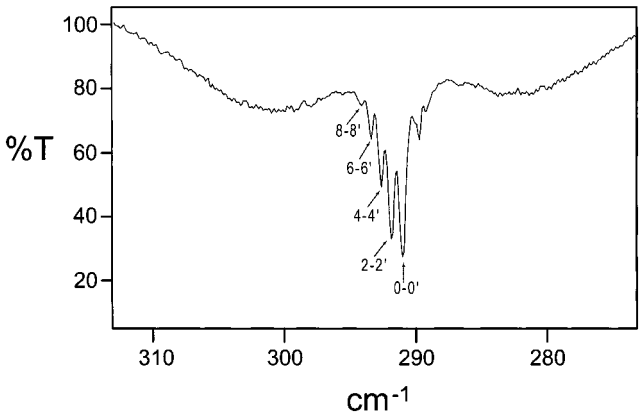

Figure 7. Far-infrared spectrum of 1,3-cyclohexadiene vapor in the 273−312 cm^{-1} region. 4 Torr, 4.2 m path length, 25 °C.

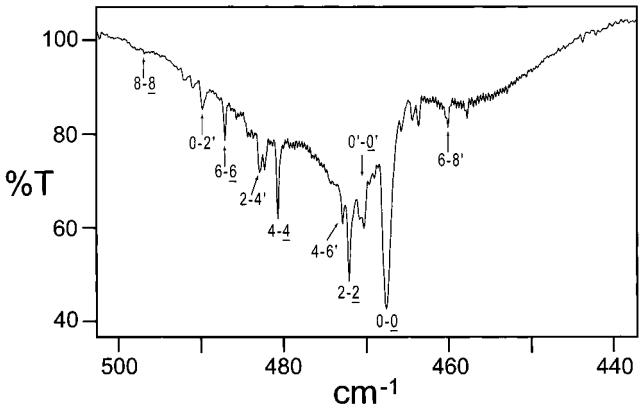

Figure 8. Infrared spectrum of 1,3-cyclohexadiene vapor in the 438−502 cm^{-1} region. 90 Torr, 20 cm path length, 25 °C. Underlined levels refer to the ν_{30} excited state; primes indicate the ν_{36} excited state.

numbers of the ν_{19} mode. A prime indicates the level is in the excited state of ν_{36}, whereas an underline indicates the excited state of ν_{30}. A double-underlined level is in the ν_{18} excited state. In later discussion a double prime indicates the second excited state of ν_{36} and an asterisk (*) indicates the excited state of ν_{35}. In Figure 4 several quadruple jump transitions (labeled $2\nu_{19}$ since these are sums of the ν_{19} frequencies below 200 cm^{-1}) can be seen in the Raman spectra. These help to confirm the transitions labeled in Figures 5 and 6 and are listed in Table 3.

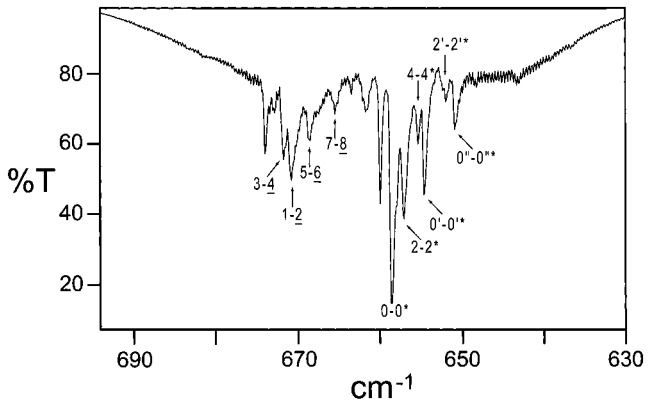

Figure 9. Infrared spectrum of 1,3-cyclohexadiene in the 630−691 cm^{-1} region. 4 Torr, 20 cm path length, 25 °C. Excited states of ν_{35} (asterisk), ν_{30}(underline), ν_{36} (prime), and $2\nu_{36}$ (double prime) are indicated with the ring-twisting (ν_{19}) quantum numbers.

TABLE 4: Calculated Ring-Puckering Barrier Heights (cm^{-1}) of 1,3-Cyclohexadiene

basis set	basis functions	barrier height[a]
6-31G*	106	1337
6-31G**	130	1332
6-311G*	132	1472
6-311G**	156	1509
6-311+G*	156	1588
6-311G(2d,p)	186	1197
6-311++G**	188	1593
6-311+G(2d.p)	210	1285
6-311G(2df,2pd)	292	1245
6-311+G(2df,2pd)	316	1299
6-311+G(3df,3pd)	370	1385
cc-pVDZ	124	1344
cc-pVTZ	292	1226
experimental	—	1132

[a] Single point energy calculations performed at the respective MP2(full)/6-31G* geometry.

Figure 7 shows the infrared spectrum in the 273−312 cm^{-1} region. Several ν_{36} bands originating from the five lowest ν_{19} states can be seen at 291.0, 291.8, 292.6, 293.4, and 294.2 cm^{-1}. In Figure 8 numerous bands involving ν_{30} can be seen. Also shown are several $\nu_{19}+\nu_{36}$ bands (such as 0−2'), and these are listed in Table 3. Figure 9 shows the ν_{35} band originating from several different ring-twisting (ν_{19}) excited states. Four

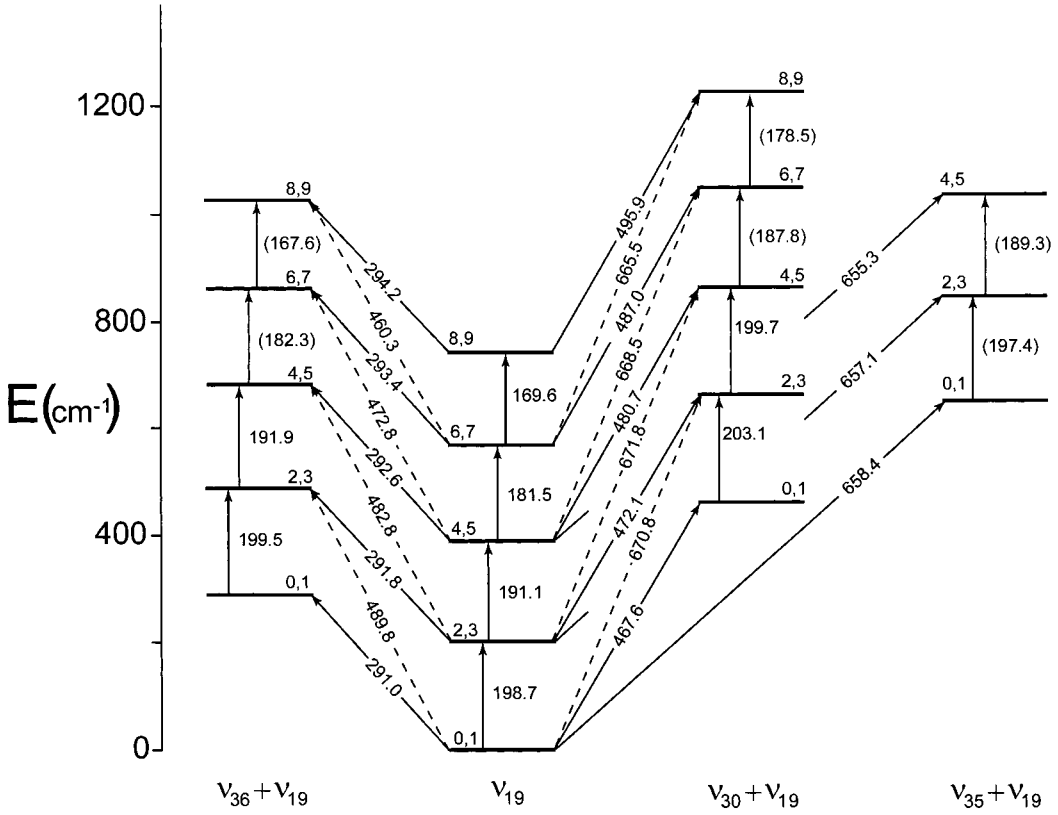

Figure 10. Energy diagram and transitions involving ν_{19}, ν_{30}, ν_{35}, and ν_{36}.

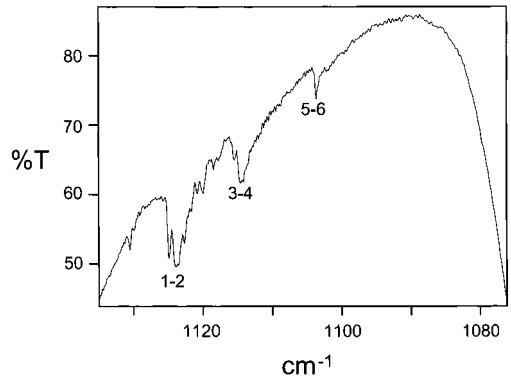

Figure 11. Mid-infrared combination bands of 1,3-cyclohexadiene. 90 Torr, 4.2 m path length, 25 °C.

$\nu_{19} + \nu_{30}$ sum bands can also be seen, and these are listed in Table 3. Figure 10 shows an energy diagram depicting many of the transitions shown in Figures 4−9 and listed in Tables 2 and 3. Most of the energy levels shown are confirmed by two or more transition frequencies.

Evidence for the ring-twisting transitions can also be seen in the mid-infrared spectra from combination bands with ν_{33} at 926.1 cm^{-1} recorded with use of a long-path cell. Three bands are listed in Table 3 and can be seen in Figure 11.

Ring-Twisting Potential Energy Function

The one-dimensional Hamiltonian used to fit the observed transitions for the various ν_{19} quantum states is

$$\mathscr{H} = \frac{-\hbar^2}{2}\frac{\partial}{\partial\tau}g_{44}(\tau)\frac{\partial}{\partial\tau} + V(\tau) \qquad (4)$$

where g_{44} is given in eq 3 and

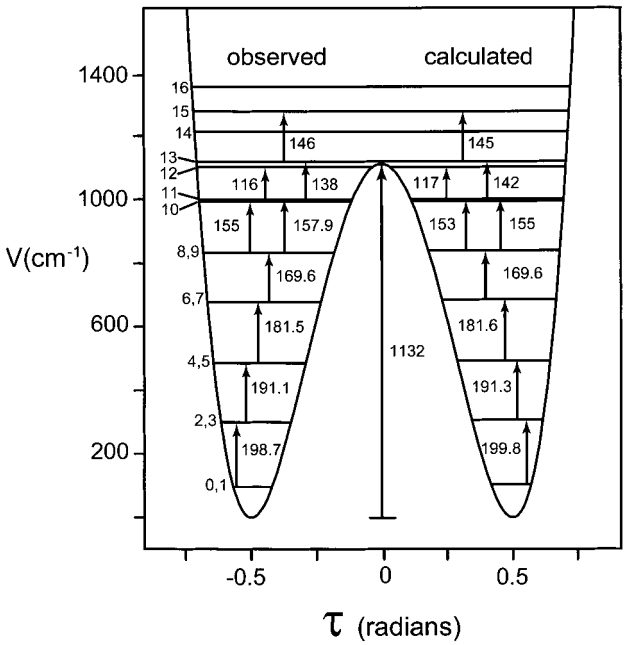

Figure 12. Ring-twisting potential energy function of 1,3-cyclohexadiene.

$$V = a\tau^4 + b\tau^2 \qquad (5)$$

Computational methods[12−16] previously described were used to adjust parameters a and b and the following potential function was determined

$$V\,(\mathrm{cm}^{-1}) = 1.845 \times 10^4\tau^4 - 9.138 \times 10^3\tau^2 \qquad (6)$$

where τ (rad) is defined in eq 2. This function along with the observed and calculated transition frequencies is shown in Figure

TABLE 5: Structural Parameters for 1,3-Cyclohexadiene

structural parameters	electron diffraction			microwave	HF[a]					experimental
	DT[c]	TR[d]	OBe	BU[f]	SB[g]	SR[h]	HF[b]	MP2[b]	B3LYP[b]	(this work)
C_1–C_2	1.468	1.465	1.468	1.47	1.471	1.476	1.475	1.466	1.466	—
C_2–C_3	1.339	1.348	1.350	1.34	1.321	1.322	1.325	1.353	1.341	—
C_3–C_4	1.494	1.519	1.523	1.50	1.516	1.519	1.510	1.509	1.510	—
C_4–C_5	1.510	1.538	1.534	1.50	1.547	1.544	1.532	1.530	1.538	—
C_2–H_8	1.07	1.099	1.082	1.086	1.071	1.073	1.076	1.087	1.085	—
C_3–H_9	1.07	1.099	1.082	1.086	1.071	1.073	1.077	1.088	1.085	—
C_4–H_{10}	1.14	1.111	1.096	1.10	1.086	1.088	1.086	1.098	1.102	—
a	121.6	120.3	120.1	120.2	121.0	120.7	120.6	120.1	120.7	—
b	118.2	120.3	120.1	120.2	121.0	120.5	120.5	119.4	120.3	—
g	111.5	110.9	110.7	110.5	112.0	109.5	111.6	110.2	111.7	—
T	99	—	114.1	109.5	—	—	106.5	107.2	106.1	—
$\angle C_3C_4C_5C_6$	—	46	—	45	38.7	44.2	42.2	50.5	43.0	43.4
$\angle C_6C_1C_2C_3$	17	18.0	18.3	17.5	13.5	15.2	14.5	17.2	14.5	14.2
τ_1	—	—	—	—	—	—	9.3	11.1	9.3	9.1
τ_3	—	—	—	—	—	—	29.5	35.1	29.8	30.1

[a] 3-21G basis set. [b] 6-31++G** basis set (this work). [c] Reference 3. [d] Reference 4. [e] Reference 5. [f] Reference 1. [g] Reference 7. [h] Reference 8.

TABLE 6: Vibrational Assignments of 1,3-Cyclohexadiene[e]

				infrared			Raman		
	C_{2v}	C_2	description	vapor	vapor[a]	liquid[a]	vapor	liquid	ab initio[c,d]
A_1	1	1	C−H sym. str.	3050.6 m	3050 m	3056 w	3052 (97)[b]	3055 p	3076 (23, 175)
	2	2	C−H sym. str.	—	—	3039 m	—	3042 p	3053 (5, 81)
(A)	3	3	CH_2 sym. str.	2950.1 m	2942 m	2939 m	2949 (52)	2939 p	2944 (40, 68)
	4	5	C═C stretch	1579.0 vw	1577 w	1578 w	1580 (100)	1578 p	1574 (2, 100)
	5	6	CH_2 deformation	1443.6 s	1444 s	1437 s	1443 (4)	1437 p	1447 (6, 5)
	6	7	C−H wag	1406.5 vw	—	1410 m	1406 (1)	1405 p	1402 (2, 6)
	7	8	CH_2 wag	1329.9 m	1330 m	1326 m	1328 (3)	1325 p	1323 (1, 3)
	8	9	C−H wag	1242.9 s	1243 s	1241 s	1242 (16)	1241/1223 p	1232 (10, 8)
	9	11	ring stretch	1058.3 m	1059 m	1057 m	1058 (4)	1057 p	1042 (2, 2)
	10	14	ring stretch	944.9 m	945 m	945 m	944 (1)	945 p	943 (2, 7)
	11	15	ring stretch	849.0 vw	850 w	848 w	849 (50)	849 p	841 (1, 10)
	12	17	ring bend	557.8 vw	559 vw	559 vw	557 (2)	559 p	549 (0.2, 2)
A_2	13	4	CH_2 antisym. str.	—	—	—	—	—	2910 (32, 163)
	14	10	CH_2 twist	—	—	—	1153 (6)	1150 p	1135 (0, 2)
(A)	15	12	CH_2 rock	1021.4 vw	1008 m	1018 w	1020 (16)	1017 p	1016 (5, 4)
	16	13	C−H wag	—	—	—	951 (4)	—	947 (0, 2)
	17	16	C−H wag	762.9 vw	753 w	—	762 (0.5)	755 p	749 (4, 0.3)
	18	18	ring twisting	—	—	506 vw	505 (2)	506 p	508 (0.2, 1)
	19	19	ring puckering	198.7 vw	—	—	199 (2)	201 d	199 (0.5, 1)
B_1	20	20	C−H antisym. str	3050 m	3050 m	3056 w	—	—	3067 (49, 19)
	21	21	C−H antisym. str	—	—	—	—	3004 d	3046 (1, 24)
(B)	22	23	CH_2 sym. str.	2883.6 m	2884 m	2874 m	2882 (8)	2873 d	2911 (50, 33)
	23	24	C═C stretch	1604.1 m	1602 m	1604 m	—	1603 p? sh	1639 (0, 1)
	24	25	CH_2 deformation	1430.9 s	1435 vs	1426 s	1431 (3)	1426 d	1437 (9, 9)
	25	26	C−H wag	1375.7 m	1377 m	1372 s	—	1373 d	1367 (4, 0.1)
	26	27	CH_2 wag	1311.3 w	—	1316 vw	—	—	1316 (1, 0.1)
	27	28	C−H wag	1165.1 vs	1165 vs	1165 s	—	1165 d	1161 (7, 1)
	28	30	ring stretch	—	—	—	956 (4)	954 d	978 (3, 0)
	29	32	ring bend	919.0 vw	—	—	—	—	914 (10, 0.3)
	30	35	ring bend	467.6 vs	468 vs	473 vs	469 (1)	473 d	456 (7, 1)
B_2	31	22	CH_2 antisym. str.	—	—	—	2948 (21)	2944 d	2952 (4, 45)
	32	29	CH_2 twist	1177.9 s	1178 s	1177 m	1178 (3)	1177 d	1144 (2, 11)
(B)	33	31	CH_2 rock	926.1 s	927 vs	924 vs	927 (1)	923 d	930 (3, 1)
	34	33	C−H wag	744.6 s	745 s	748 vs	744 (0.2)	748 d	725 (16, 0.2)
	35	34	C−H wag	658.4 vs	658 vs	657 vs	657 (0.5)	658 d	653 (100, 1)
	36	36	ring twisting	291.0 s	—	—	292 (2)	298 d	292 (2, 2)

[a] Reference 23. [b] Relative intensity in parentheses. [c] Frequency scaled with a scaling factor of 0.9613. [d] Relative intensities (IR, Raman). [e] Abbreviations: s, strong; m, medium; w, weak; v, very; sh, shoulder; p, polarized; d, depolarized.

12. The frequencies are also listed in Table 2 where they are compared with the previously reported values. The potential function has a barrier of 1132 cm^{-1} and the energy minima are at $\tau = \pm 0.498$ rad (28.5°). This corresponds to twisting angles of $\tau_1 = 9.1°$ and $\tau_3 = 30.1°$. The previous Raman study[6] concluded that the inversion barrier was 1099 cm^{-1}. This was a relatively imprecise extrapolation but fortuitously produced a reasonably good value. The previous study was not able to determine the dihedral angles because the reduced mass had not been calculated.

Ab Initio Calculations

Ab initio calculations were carried out utilizing a variety of basis sets. Table 4 lists these along with the barrier calculated for each case. Figure 13 shows the structure for the MP2/6-311++G** calculation, and Table 5 compares the structural

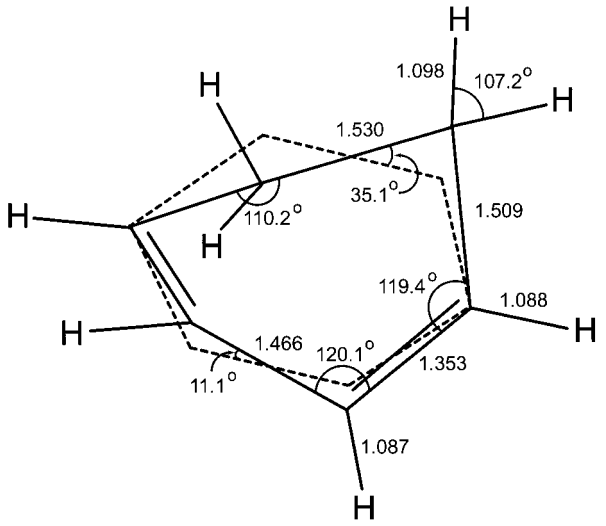

Figure 13. Calculated structure for 1,3-cyclohexadiene using the MP2 method with a 6-311++G** basis set.

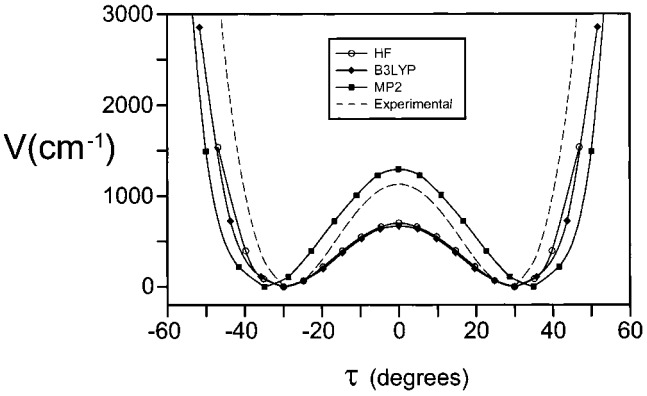

Figure 14. Comparison of experimental and calculated potential energy curves for the ν_{19} ring-twisting mode of 1,3-cyclohexadiene. The calculations used a 6-31G* basis set.

parameters with those from previous work. All of the calculations give similar structures. The τ_3/τ_1 ratio for the various calculations ranged from 3.152 to 3.273. The latter value from the MP2/6-311++G** calculation was used for the kinetic energy computation. This parameter is not very critical for a meaningful structure determination.

Table 6 compares the calculated vibrational frequencies and intensities for the MP2/6-31G* basis set with the infrared (vapor) and Raman (liquid) frequencies recorded in this study and with experimental values reported previously.[22] The agreement is very good after several of the original vibrations are reassigned. It is also interesting to compare the experimental potential energy function with ones calculated by different ab initio methods. Figure 14 shows this comparison. Each of the calculations does a reasonably good job of calculating the energy minima, but the calculation of the barrier height is less accurate. The Hartree−Fock (HF) and density functional (B3LYP) calculations give poor (too low) barrier values, whereas the MP2 calculation is considerably closer. Nonetheless, all MP2 calculations (Table 4) result in barriers that are somewhat too high.

Discussion

In the present work both accurate determinations of the inversion barrier (1132 cm^{-1} or 3.23 kcal/mol) and the twisting angles (30.1° and 9.1°) have been achieved for the first time. The ab initio calculations all predict barriers that are somewhat too high. The barriers from these calculations assume that the molecule must pass through a planar structure to invert. Since the molecule can invert through changes in τ_1 and τ_3 without exactly going through the planar form, it can likely find a way to do this over a somewhat lower barrier (1132 cm^{-1}) than computed.

Despite some expected conjugation, 1,3-cyclohexadiene takes on a nonplanar structure to reduce the CCC angles γ at the CH_2 groups to 110.2°. In a planar form these angles would be close to 120°. The twisting of the ring also reduces the $-CH_2-CH_2-$ torsional interaction.

The determination of the one-dimensional potential energy function in eq 6 was based on the assumption that the other vibrational modes do not interact with ν_{19}. Examination of Figure 10 shows that this is a reasonable approximation, but that there is a degree of interaction. The $1 \rightarrow 2$ transition at 198.7 cm^{-1} shifts to 199.5 cm^{-1} in the excited state of ν_{36}, to 203.1 cm^{-1} in the excited state of ν_{30}, and to 197.2 cm^{-1} in the excited state of ν_{35}. The frequency shifts each reflect the degree of interaction. This is largest for the ν_{30} ring-angle-bending mode, and the two vibrations are anticooperative when the vibrations are simultaneously excited. Both ν_{19} and ν_{30} are governed to a large extent by angle-bending force constants, so this interaction is not surprising. There is very little interaction between ν_{19} and ν_{36} at 291 cm^{-1} even though both are out-of-plane motions, presumably because of the difference in symmetry. There is also no evidence for significant interaction between ν_{19} and the other out-of-plane ring mode ν_{18} at 506 cm^{-1} since their frequency separation is quite substantial.

Acknowledgment. The authors thank the National Science Foundation, the Texas Advanced Research Program, and the Robert A. Welch Foundation for financial assistance.

References and Notes

(1) Butcher, S. S. *J. Chem. Phys.* **1965**, *42*, 1830.

(2) Luss, G.; Harmony, M. D. *J. Chem. Phys.* **1965**, *43*, 3768.

(3) Dallinga, G.; Toneman, L. H. *J. Mol. Struct.* **1967**, *1*, 11.

(4) Traetteberg, M. *Acta Chem. Scand.* **1968**, *22*, 2305.

(5) Oberhammer, H.; Bauer, S. H. *J. Am. Chem. Soc.* **1969**, *91*, 10.

(6) Carreira, L. A.; Carter, R. O.; Durig, J. R. *J. Chem. Phys.* **1973**, *59*, 812.

(7) Saebø, S.; Boggs, J. E. *J. Mol. Struct.* **1981**, *73*, 137.

(8) Sygula, A.; Rabideau, P. W. *J. Mol. Struct. (THEOCHEM)* **1992**, *262*, 117.

(9) Laane, J.; Lord, R. C. *J. Chem. Phys.* **1967**, *47*, 4941.

(10) Laane, J.; Lord, R. C. *J. Chem. Phys.* **1968**, *48*, 1508.

(11) Laane, J. *Appl. Spectrosc.* **1970**, *24*, 73.

(12) Laane, J. *J. Phys. Chem.* **2000**, *33*, 7715.

(13) Laane, J. *Pure Appl. Chem.* **1987**, *59*, 1307.

(14) Laane, J. In *Structures and Conformations of Non-Rigid Molecules*; Laane, J., Dakkouri, M., van der Veken, B., Oberhammer, H., Eds.; Amsterdam, 1993; Chapter 4.

(15) Laane, J. *Annu. Rev. Phys. Chem.* **1994**, *45*, 179.

(16) Laane, J. *Int. Rev. Phys. Chem.* **1999**, *18*, 301.

(17) Haller, K.; Chiang, W.-Y.; del Rosario, A.; Laane J. *J. Chem. Phys.* **1996**, *379*, 19.

(18) Laane, J.; Harthcock, M. A.; Killough, P. M.; Bauman, L. E.; Cooke, J. M. *J. Mol. Spectrosc.* **1982**, *91*, 286.

(19) Harthcock, M. A.; Laane, J. *J. Mol. Spectrosc.* **1982**, *91*, 300.

(20) Schmude, R. W.; Harthcock, M. A.; Kelly, M. B.; Laane, J. *J. Mol. Spectrosc.* **1987**, *124*, 369.

(21) Tecklenburg, M. M.; Laane, J. *J. Mol. Spectrosc.* **1989**, *137*, 65.

(22) Strube, M. M.; Laane, J. *J. Mol. Spectrosc.* **1988**, *129*, 126.

(23) Di Lauro, C.; Neto, N.; Califano, S. *J. Mol. Struct.* **1969**, *3*, 219.